MinnesotaCorn RESEARCH & PROMOTION COUNCIL

PROGRESS REPORT

PROJECT TITLE: Sustainable polyesters from corn as tomorrow's advanced plastics
PROJECT NUMBER: 6096-23DD
REPORTING PERIOD: 1 July – 30 September 2023
PRINCIPAL INVESTIGATOR: Marc A. Hillmyer
ORGANIZATION: University of Minnesota
PHONE NUMBER: 612.625.7834
EMAIL: hillmyer@umn.edu

---

(1) Structure and Performance of Stretched PLA Films

1.1) PROJECT ACTIVITIES COMPLETED DURING THE REPORTING PERIOD.

Poly(lactide) (PLA) is a sustainable alternative for use in plastics packaging, owing to its corn-based feedstock. This work continues to explore the benefits of blending an amphiphilic block polymer, poly(ethylene oxide)-block-poly(butylene oxide) (PEO-PBO), commercial tradename FORTEGRA, with semicrystalline poly(lactide) (PLLA) for the purposes of improving mechanical integrity in uniaxially stretched films. We have previously investigated how uniaxially drawn PLLA is mechanically influenced by blending with 3 wt % PEO-PBO, studying such parameters as material toughness and crystallinity in relation to strain rate and drawing ratio. This report expands upon those results by probing crystallite structure directly using X-ray scattering, a valuable complement to thermal characterization of crystallinity previously reported.

1.2) IDENTIFY ANY SIGNIFICANT FINDINGS AND RESULTS OF THE PROJECT TO DATE.

Materials and methods: Semicrystalline grade PLLA (4032D) was purchased from NatureWorks and blended with 3.0 wt % PEO-PBO through a masterbatch dilution method. Amorphous, isotropic sheets were compression molded, and stretched to a target stretching ratio (λ) at 70°C. This temperature is selected to isolate the effects of strain induced crystallization from thermally induced crystallization. The stretching ratio is given by:

$$\lambda = \frac{L}{L_0}$$

where L is the final film length and L_0 is the initial film length. Films were rapidly quenched to room temperature after stretching. The stretched films are labeled as S-(N/B)-Uλ_x where S stands for semi-crystalline grade PLLA, N/B indicates either neat PLLA (N) or 3.0 wt% PEO-PBO (B), U stands for uniaxial stretching, λ is the stretching ratio, and x is the stretching rate (%/sec). For example, $SNU4_{10}$ stands for a neat semicrystalline PLLA film uniaxially stretched to λ = 4 at 10% strain/second. Two-dimensional wide-angle X-ray scattering (WAXS) patterns were obtained for all films using a Ganesha 300 XL (SAXSLAB) using an X-ray wavelength of 1.54 Å. One-dimensional (1D) traces were obtained by integration across the entire azimuthal angle range.

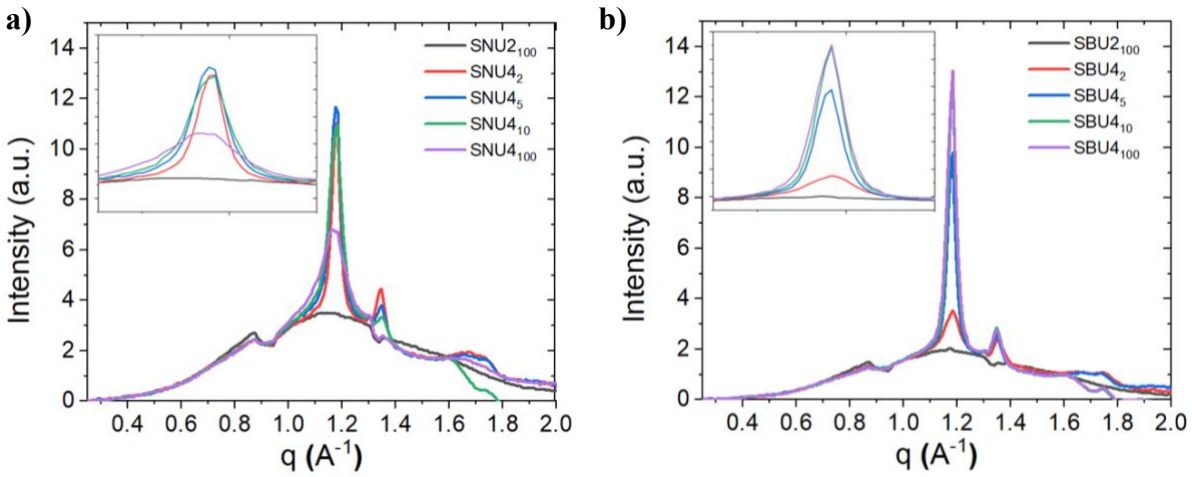

Figure 1. Wide angle X-ray scattering of (a) neat PLLA and (b) PEO-PBO/PLLA films stretched to $\lambda = 2$ or 4 at stretching rates ranging from 2 to 100 $\%s^{-1}$. The inset shows the (200)/(110) peak at $q = 1.19$ Å^{-1} in more detail.

Impact of stretching on crystallinity: Wide angle X-ray scattering (WAXS) experiments were performed on PLLA and PEO-PBO/PLLA stretched films in order to gain a better understanding of the impact of stretching ratio and rate on crystal structure. **Figure 1** shows the azimuthally integrated 1D WAXS data for both PLLA and PEO-PBO/PLLA films stretched to $\lambda = 2$ or 4 at stretching rates varying from 2 to 100 % s^{-1}. Both PLLA and PEO-PBO/PLLA films stretched to $\lambda = 2$ (SNU2$_{100}$ and SBU2$_{100}$) exhibit only an amorphous halo, with little evidence of crystallinity in WAXS. All films stretched to $\lambda = 4$ exhibit significant evidence of crystallinity, most prominently peaks associated with the (200)/(110) and (203) planes of the PLLA crystal unit cells at $q = 1.19$ Å^{-1} and $q = 1.35$ Å^{-1}, respectively. However, the relationship between stretching rate and crystallinity is starkly different in PLLA versus PEO-PBO/PLLA films. In neat PLLA films, the crystallinity decreases with increasing stretching rate, evidence by the decreasing intensity of the (200)/(110) crystal peak. By contrast, in PEO—PBO/PLLA films, the crystal peak intensity increases with increasing stretching rate. This difference is likely due both to the ability of the PEO-PBO particles to nucleate crystals and to the partial miscibility of PEO-PBO with PLLA which plasticizes the PLLA matrix. Thus, the combined effect of heterogeneous nucleation and plasticization enhances the crystallization kinetics of PLLA in the blends.

Impact of stretching on crystal size: In addition to the difference in the relationship between crystallinity and stretching rate, PLLA and PEO-PBO/PLLA films also exhibit a difference in crystal size as a function of stretching rate. This is evidenced by broadening of the (200)/(110) peak, which is shown in more detail in the inset figures of **Figure 1**. In PLLA films, significant peak broadening is observed with increasing stretching rate, while in the PEO-PBO/PLLA films peak breadth is relatively unaffected by stretching rate. The Scherrer equation gives an inverse relationship between mean crystallite size and peak breadth, suggesting that average crystallite size decreases in PLLA but remains constant in PEO-PBO/PLLA blends with increasing stretching rate.

---

(2) Mechanically Tough Bulk PLA

2.1) PROJECT ACTIVITIES COMPLETED DURING THE REPORTING PERIOD.

Poly(lactide) (PLA) is an industrially compostable commercial polymer, which is produced from corn-based feedstocks. Production of PLA emits significantly less greenhouse gases than traditional polyolefins, making it a sustainable alternative to many commodity polymers. Unfortunately, PLA applications are

restricted by the material's inherent mechanical limitations, such as low tensile toughness. To address this concern, we are studying how mechanical properties of diblock polymers influence their capacity to toughen PLA, enabling design of commercially relevant materials which are > 95% PLA. Specifically, we have reported the tensile toughness of a PLA modified by a series of poly(isoprene)-block-poly(ethylene oxide) (PI-*b*-PEO) diblock polymer additives to understand how solid-like vs. liquid-like behavior of a specific additive influences toughening efficacy. This report expands on previous results of PLA toughening strategies via blending with diblock polymers.

2.2) IDENTIFY ANY SIGNIFICANT FINDINGS AND RESULTS OF THE PROJECT TO DATE.

Materials and methods: PI-*b*-PEO diblock polymer was synthesized as described previously. The diblock studied in this report has molecular weight (M_n) of 3,350 g/mol and ethylene oxide volume fraction (f_{EO}) of 0.35, as determined through ^{1}H NMR spectroscopy, and dispersity ($Đ$) of 1.10, as determined using size exclusion chromatography (SEC). Blends of PI-*b*-PEO and PLA were prepared through a masterbatch dilution technique to achieve a 5.0 wt % blend of PI-*b*-PEO in PLA. Samples were compression molded at 135 °C, quenched as specified, cut into dogbone specimens, and tested at a strain rate of 1 mm/min after two days of aging at room temperature. Thermal properties were quantified using differential scanning calorimetry at a heating rate of 10 °C/min.

Effect of PI-b-PEO on mechanical properties of PDLLA: The PI-*b*-PEO diblock polymer was previously shown to toughen PLA. This is hypothesized to be due in part to a liquid-like behavior at room temperature, which enables the diblock polymer to drain through propagating crazes. Changing the degree of crystallinity of PEO ($X_{C,\,PEO}$) can yield a more solid-like or liquid-like material, providing a means of testing this hypothesis. One method of controlling $X_{C,\,PEO}$ is by changing the temperature at which pressed films are quenched. Pursuant to this, pressed films were quenched either using a cold press at 10 °C or by submerging in liquid nitrogen to crystallize the PEO block. DSC traces of film quench using these methods are shown in **Figure 2a**. Quenching the PI-*b*-PEO/PLA film immediately after pressing with a cold press does not crystallize PEO, while subsequently soaking the film in liquid nitrogen crystallizes PEO as evident through the melting exotherm. This demonstrates that soaking a film in liquid nitrogen will crystallize PEO within the PLA blends. Notably, the PEO crystallites will not melt at room temperature (T_m = 35 °C), enabling tensile testing of PLA blends with both semicrystalline and purely amorphous diblock polymer.

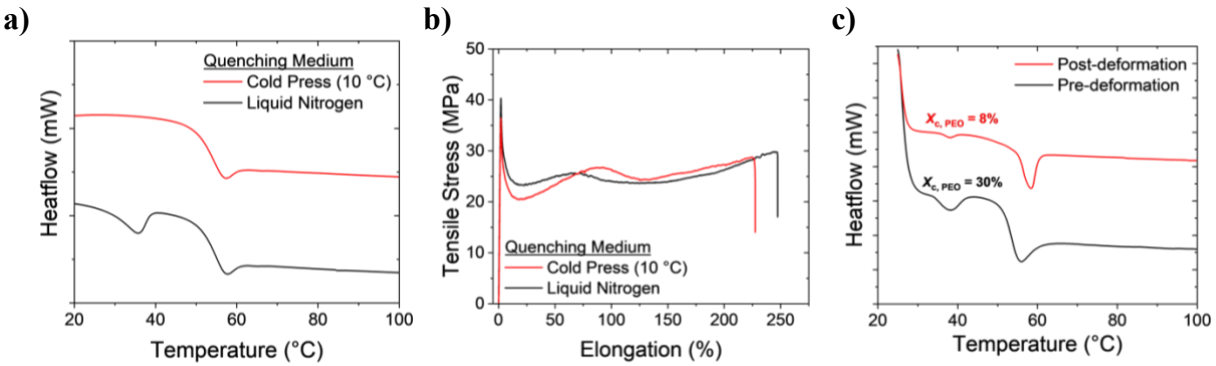

Figure 2. a) DSC First heating traces of films quenched with water and liquid nitrogen. b) Stress-strain curves of PLA blend with different quench mediums. c) DSC First heating traces of films quenched with liquid nitrogen before and after mechanical testing.

Following different quenching protocols, tensile experiments were performed on PLA blends after two days of aging under ambient conditions. Representative stress-strain curves are shown in **Figure 2b** for PLA blends quenched using both a cold press and liquid nitrogen. The mechanical integrity is unchanged by the quench method, suggesting that PEO crystallinity does not inherently impact the diblock polymer's capacity to effectively toughen PLA. Interestingly, the diblock polymer may still behave as a liquid despite

crystallization. Representative DSC traces of undeformed and deformed tensile bars are shown in **Figure 2c**. The deformed bars show a reduction in magnitude of the PEO melting peak corresponding to a three-fold decrease in X_C, suggesting that mechanical melting of the PEO crystallites occurs during deformation. Therefore, PEO crystallinity is not an inherent barrier to effective toughening, as the mechanical melting of the diblock copolymer allows for liquid-like behavior during tensile deformation.

---

(3) Thermally Resistant High-Impact Poly(L-lactide)-based Triblock Copolymers

3.1) PROJECT ACTIVITIES COMPLETED DURING THE REPORTING PERIOD.

In our previous report, we presented preliminary data on a new research thrust targeting toughened blends of poly(L-lactide) (PLLA) and poly(γ-methyl-ε-caprolactone) (PγMCL). By compatibilizing these two immiscible polymers with a PDLA-*b*-PγMCL-*b*-PDLA (DMD) triblock polymer, we aim to simultaneously improve stress transfer between the blend constituents and accelerate PLLA crystallization using PLLA-PDLA stereocomplexes as nucleating agents. Initial 80/20 w/w blends of a commercial PLLA (Natureworks 4032D) with 21-kg/mol PγMCL produced little to no tensile toughness enhancement, and poor properties were still observed even after the addition of 2 wt % DMD. To remedy this, we planned to optimize the viscosity of the PγMCL molar mass using well-established relations describing the conditions for the formation of co-continuous rubbery phase morphologies, which are generally associated with the best mechanical properties. This report details the required rheological measurements and the tensile properties of pristine 80/20 blends of 4032D pellets with PγMCL with two new molar masses.

3.2) IDENTIFY ANY SIGNIFICANT FINDINGS AND RESULTS OF THE PROJECT TO DATE.

Figure 3 below shows a plot of zero-shear viscosity (η_0) versus weight-average molar mass (M_w) for various PγMCLs used for rheological screening. Zero-shear viscosities were calculated by linearly extrapolating the stable viscosity plateau in a steady shear experiment back to zero shear rate. M_w was calculated using two different light scattering angles (right-angle, "RALS," and low-angle, "LALS") in size exclusion chromatography, and both datasets and their fits are shown. The scaling exponents agree reasonably well with the reptation theory prediction $\eta_0 \sim M_w^3$ and the generally observed scaling $\eta_0 \sim M_w^{3.4}$. Co-continuity of host and rubbery phases is predicted when $\varphi_1 / \eta_1 = \varphi_2 / \eta_2$, where φ and η are the volume fraction and viscosity of each species.[1] The zero-shear viscosity of 4032D pellets was measured to be 2856 Pa * s, and using the densities of the two components (1.27 g/cm^3 for moderately crystalline PLLA, 1.037 g/cm^3 for PγMCL), a prediction for the ideal molar mass of PγMCL was predicted. The RALS dataset gave M_w = 121 kg/mol, and the LALS dataset gave M_w = 145 kg/mol. Averaging these values and dividing by the typical dispersity of 1.2 gave the number-average molar mass (M_n) target for PγMCL synthesis, 111 kg/mol. A difunctional PγMCL was then synthesized using methods previously described, yielding M_n = 103 kg/mol. M_w measurement from SEC has not yet been performed due to column issues.

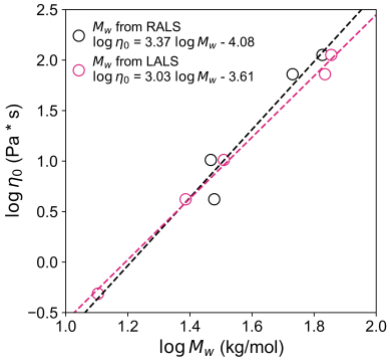

Figure 3. Plot of η_0 v. M_w for various PγMCLs with log-log fits overlaid with the data. The numerical results of the fits are shown in the top left corner.

Figure 4 below compares the stress-strain curves of the blends of 4032D pellets with the PγMCLs synthesized thus far after having been rapidly quenched from the melt after compression molding at 190 °C. The behavior of the 21-kg/mol PγMCL blend is reproduced in **Figure 4a**, while the tensile behavior of the blends with the two new PγMCL molar masses is shown in **Figures 4b-c**. In **Figure 4c**, "no-I" PγMCL refers to the use of no exogeneous initiator for the synthesis, targeting the highest possible molar mass for the γMCL feedstock. The 103-kg/mol PγMCL blend exhibits slightly more consistent ductility improvements over neat PLLA (4% typical strain at break) than the 21-kg/mol batch, and the plateau stress recorded during next elongation is reduced from ~30 to ~25 MPa, indicating that the PLLA matrix shear-yield more easily with a higher molar mass of PγMCL. Moving to even larger PγMCL molar masses produces an abrupt increase in ductility, reduces the yield stress by ~3 MPa, and further reduces the plateau stress to ~23 MPa, demonstrating greatly improved stress transfer from the matrix to the PγMCL domains. Given that the "no-I" PγMCL molar mass likely greatly exceeds the threshold required for the co-continuous criterion, it is puzzling that this material produces the best tensile properties. In future work, the new blends will be compatibilized with DMD triblock to examine the potential gains in toughness and strength, and scanning electron microscopy will be used to morphologically rationalize the results.

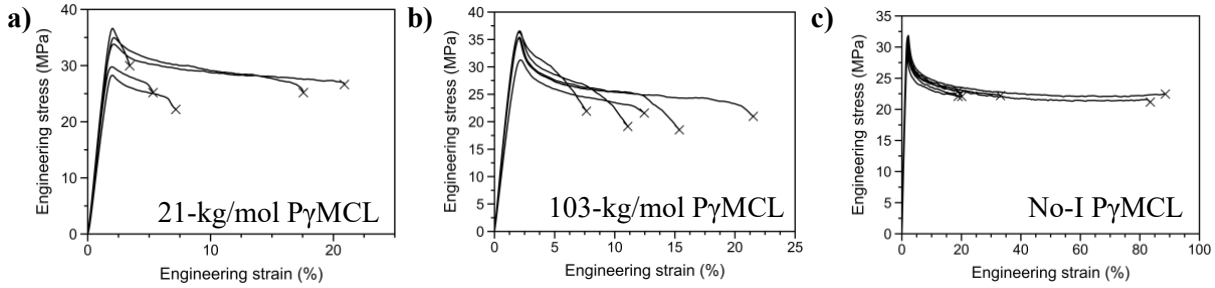

Figure 4. Stress-strain curves for pristine 80/20 PLLA/PγMCL blends for the range of PγMCL molar masses so far synthesized.

References

1. Jordhamo, G. M.; Manson, J. A.; Sperling, L. H., Phase Continuity and Inversion in Polymer Blends and Simultaneous Interpenetrating Networks. *Polym Eng Sci* **1986,** *26* (8), 517-524.

---

(4) Development of a new strategies for polymerizing oleyl alcohol

4.1) PROJECT ACTIVITIES COMPLETED DURING THE REPORTING PERIOD.

During the previous quarter we have focused on wrapping up our paper on catalyst control of polyester branching through the hydroesterificative polymerization of 10-undecen-1-ol. We have also further explored the methoxy carbonylation of oleyl alcohol as a precursor for condensation polymerization.

4.2) IDENTIFY ANY SIGNIFICANT FINDINGS AND RESULTS OF THE PROJECT TO DATE.

While mixed ligand data had already been collected, comparison experiments under identical conditions had not been conducted. Full ^{1}H NMR and SEC data was collected for the three main ligands used in the paper. Regardless of ligand choice, conversion did not exceed 82%. While we have successfully obtained materials with a range of % branching, SEC shows that molar mass remains relatively low, specifically for these unoptimized mixed ligand systems. This further demonstrates the need for more extensive reaction optimization depending on the ligand(s) used. We also conducted polymerization of 10-undecenol using the optimized conditions for P(furyl)$_3$ and found the standard deviation of % branching to be 2%.

Table 1: Hydroesterificative polymerization of 10-undecen-ol with mixed ligand systems

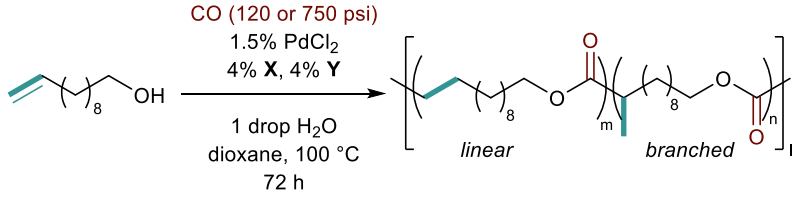

Ligand X	Ligand Y	Conv. (%)[b]	Yield[c]	Branching[d] (%)	M_n (Đ)
PPh_3[e]	PPh_3	79	76	26	3.2 (1.3)
PPh_3[e]	P(furyl)$_3$	70	79	42	2.5 (1.3)
P(furyl)$_3$[e]	P(furyl)$_3$	80	80	46	3.6 (1.4)
PPh_3[f]	P(*o*-OMePh)$_3$	75	71	55	4.2 (1.3)
P(furyl)$_3$[f]	P(*o*-OMePh)$_3$	76	69	61	1.7 (1.4)
L2[f]	P(*o*-OMePh)$_3$	82	89	78	7.5 (1.1)

[a]Reaction conditions: 1.67 M monomer in dioxane, 1.5% $PdCl_2$, 1 drop H_2O, 4% each ligand; 100 °C and 72 h. [b]calculated from alcohol end group. [c]*in situ* ^{1}H NMR yield calculated via DMT internal standard. [d] measured by *in situ* ^{1}H NMR spectroscopy. [e]120 psig CO. [f]750 psig CO.

In an effort to expand the utility of hydroesterificative polymerization we have also been exploring oleyl alcohol as a bio-derived monomer. Despite various optimization attempts, yields remained too low to achieve polymeric material. Due to this, we have been exploring a direct methoxycarbonylation approach. Initially, oleyl alcohol was methoxycarbonylated with a 12% isolated yield on a 4.3 gram scale using 3% $PdCl_2$, 6% P(furyl)$_3$, and 8% HCl with 750 psig CO in dioxane at 75 °C for 72 hours. While promising, further screening was necessary to improve the overall yield. After exploring a few different ligands and acid additives, P(furyl)$_3$ with HCl provided the highest yield of the two methoxy carbonylated products. Running reactions in dilute methanol resulted in an ester yield of 83%. Products yields decreased with a lower catalyst loading and water has been identified as a promising acid additive. Once fully optimized, we plan to purify the methoxycarbonylated products and further explore condensation polymerization in the presence of $Ti(OBu)_4$.

Table 2: Screening of the methoxycarbonylation of oleyl alcohol

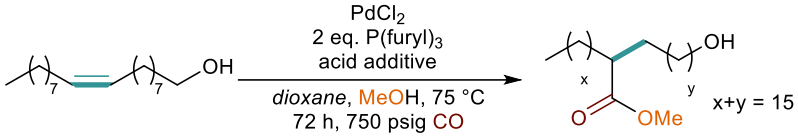

Catalyst Loading (%)	Acid Additive	MeOH eq.	Conversion (%)	Yield (%)[a]
3	8% HCl	2	71	41
3	8% HCl	7	79	67
3	8% HCl	22	95	**83**
3	8% TsOH•H_2O	2	75	33
1.5	4% HCl	7	61	52
1.5	36% H_2O	7	81	60

[a]*in situ* ^{1}H NMR yield calculated via DMT internal standard.

(5) Amorphous polyamides from biomass

5.1) PROJECT ACTIVITIES COMPLETED DURING THE REPORTING PERIOD.

We report our investigations into the water uptake characteristics of copolymer films consisting of ε-caprolactam (CLAm) and γ-methyl-ε-caprolactam (MeCLAm). Our work over the summer also involved rheological characterization of these films. Ongoing research is looking into their hydrolytic stability and potential applications as adhesives and in 3D printing.

5.2) IDENTIFY ANY SIGNIFICANT FINDINGS AND RESULTS OF THE PROJECT TO DATE.

The tensile properties presented in our previous report demonstrated the plasticizing effect of water on our polyamide films. We have studied the water uptake characteristics of these films in more detail by conditioning small specimens under different relative humidities and quantifying their equilibrium water content using thermogravimetric analysis (**Figure 5A**). The data showed water uptake of amorphous films (65, 76, and 100 mol% MeCLAm) to increase with increasing CLAm content. This is likely due to changes in the overall polarity of the polymer: the addition of methyl substituents along the chain makes the polymer less polar and therefore reduces its affinity for water. Semicrystalline PA6 was found to contain less water than a semicrystalline copolymer containing 56 mol% MeCLAm. We have previously shown that the crystallinity of copolymers decreases steadily with increasing MeCLAm content. Therefore, the lower water uptake of PA6 can be explained by a smaller volume fraction of amorphous regions being available for water absorption than in the 56 mol% copolymer.

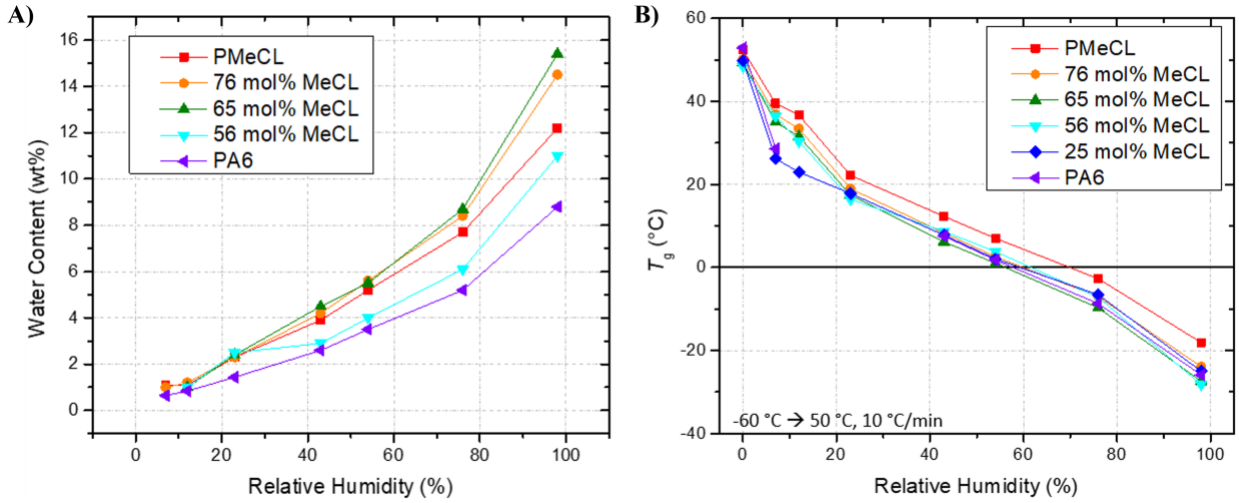

Figure 5. A) Water content of polyamide films after equilibrating at different relative humidities, quantified using thermogravimetric analysis. **B)** Influence of film hydration on the glass transition temperature (T_g) according to differential scanning calorimetry.

The conditioned films were also analyzed using differential scanning calorimetry to quantify how the presence of water influences glass transition temperature (**Figure 5B**). Dried polymer powders were used as a reference material to represent the highest achievable glass transition temperatures (0% relative humidity, T_g=48-53 °C). The highest relative humidity of 98% resulted in a 70 °C decrease in the glass transition temperature for all polymers. This plasticizing effect has important implications on the polymers' ageing and mechanical properties over time. We have observed both humidity and time-dependent crystallization behavior of copolymer films: melt-processed copolymer films containing a high percentage of MeCLAm remain amorphous when conditioned under low humidity (7%) at room temperature (20-22 °C) but undergo crystallization under high humidity (54%) if allowed to equilibrate for days or up to several weeks. These findings highlight the importance of controlling the sample environment and conditioning time in collecting reproducible characterization data.

(6) Polyesters via new chemistries of furan building blocks from corn sugars

6.1) PROJECT ACTIVITIES COMPLETED DURING THE REPORTING PERIOD.
Project activities completed are combined with findings and results described below.

6.2) IDENTIFY ANY SIGNIFICANT FINDINGS AND RESULTS OF THE PROJECT TO DATE.
Continuing our use of the furan-derived, bicyclic lactone **1** (conveniently prepared merely by mixing the corn-derived reactants itaconic anhydride and furfuryl alcohol at ambient temperature[1]), as reported in the last quarterly report, we have carried out a set of derivatization reactions that provide very efficient access to some important and potentially valuable monomers. These reactions are summarized in **Figure 6**. An important activity during the most recent quarter has been collecting the full set of publishable structural characterization [NMR spectra (proton, carbon, 1D, and 2D), infrared spectra, and high resolution mass measurements (HRMS)] *and* preparing and submitting a manuscript that is currently undergoing peer review.[2]

The most important monomers arising from this approach are the acrylate esters **3a-c** and the methacrylate esters **4a-c**. These α,β-unsaturated esters are among the most useful class of monomers. In particular, they are known to perform exceptionally well in reversible addition fragmentation chain transfer (RAFT) polymerization processes. We are now learning about their reactivity and how to handle (purify, characterize, etc.) polymers made from them under RAFT conditions. Interestingly (and proudly), the manuscript we have submitted for publication[2] is for a special issue of the journal *ARKIVOC* that will be dedicated to Professor Samir Zard, *one of the leading pioneers[3] of RAFT polymerization*!

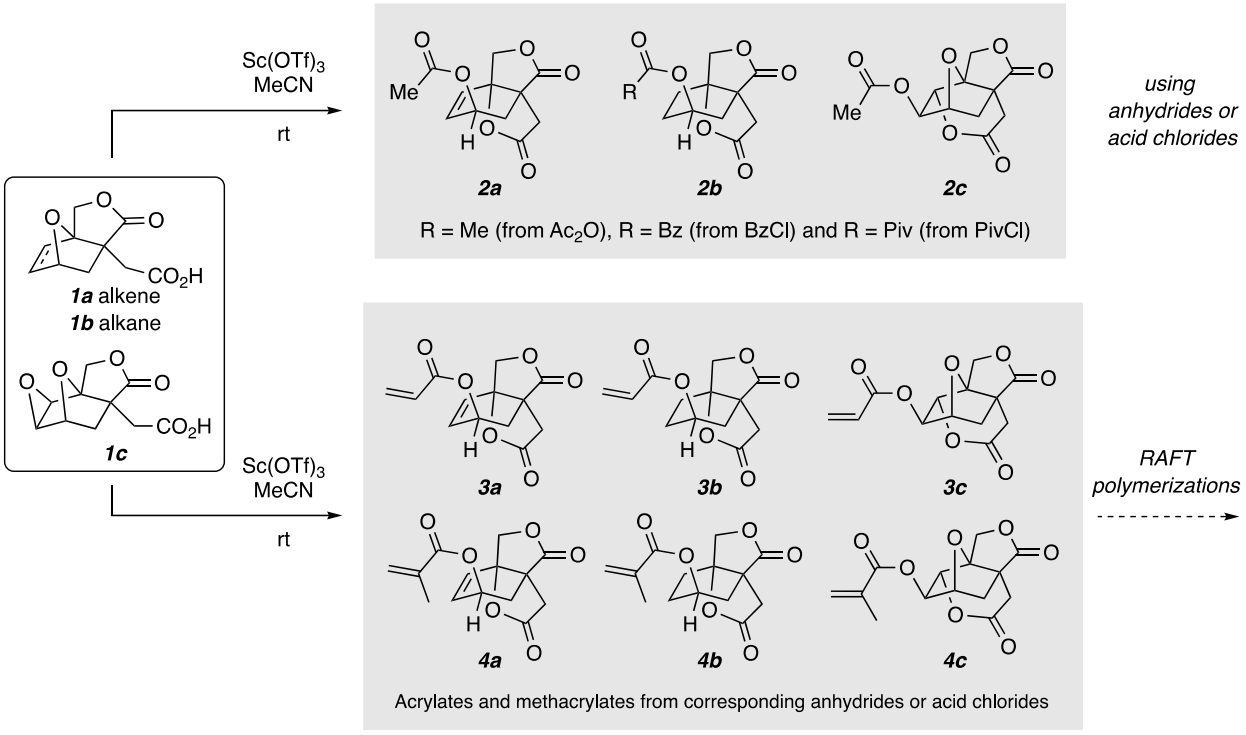

Figure 6. Successful (and efficient) preparation of a suite of methacrylate monomers (**4-6**) derived from the trivially available[1] lactone acid **1**.

References

1. Diels-Alder reactions of furans with itaconic anhydride: Overcoming unfavorable thermodynamics. Pehere, A. D.; Xu, S.; Thompson, S. K.; Hillmyer, M. A.; Hoye, T. R. *Org. Lett.* **2016**, *18*, 2584.
2. Novel conversions of a multifunctional, bio-sourced lactone carboxylic acid. Kaicharla, T.; Lee, S.; Wang, R.; Pehere, A. D.; Xu, S.; Hoye, T. R. *ARKIVOC*, submitted manuscript for special issue honoring Prof. Samir Zard.
3. (a) Corpart, P.; Charmot, D.; Biadatti, T.; Zard, S.; Michelet, D. WO9858974A1. Method for block polymer synthesis by controlled radical polymerization. **1998**. (b) Corpart, P.; Charmot, D.; Zard, S.; Biadatti, T.; Michelet, D. U.S. Patent 6,153,705. Method for block polymer synthesis by controlled radical polymerisation. **1998**.

---

(7) Use of weak solid acids for the valorization of corn-derived resources

7.1) PROJECT ACTIVITIES COMPLETED DURING THE REPORTING PERIOD.

We have evaluated the acid site density of S-zeosils using amines and variable preparation techniques, with the goal of understanding and optimizing the catalyst activity (by mass) of weak acid sites for corn-derived chemicals. While our previous experiments have identified the S-O-Z bonds to anchor weak acid sites, the acid site density was significantly lower than conventional Al sites. Our most recent goal was to evaluate the impact of steaming that could break up sulfuric acid chains (S-O-S bonds) and create high density of single S-containing species and active sites.

7.2) IDENTIFY ANY SIGNIFICANT FINDINGS AND RESULTS OF THE PROJECT TO DATE.

The loading of active sites and the co-feeding of steam was found to exhibit complex behavior consistent with interchange of S-containing sites within a zeolite micropore environment. While we know water can break up SOx species, inside the pores of the zeolite the species are in high concentration and might readily interconvert. This is supported by our results that steaming did not have a significant impact on increasing the total active site density of acid sites; there was no statistical difference between co-feeding steam and not-co-feeding steam on the butadiene formation rate from corn-derived-THF.

Moving forward, we hypothesize that the challenge is high S species loading, and we aim to vary both the total S-species loading to lower amounts and use higher surface area species where independent active sites could be stabilized, ultimately yielding higher activity per unit mass of catalyst.

3.) CHALLENGES ENCOUNTERED.

No research challenges to report.

4.) FINANCIAL INFORMATION.

No financial information to report.

5.) EDUCATION AND OUTREACH ACTIVITES.

The NSF Center for Sustainable Polymers hosted 14 undergraduate students, 9 who were housed and supported at the University of Minnesota. They participated in active research within the NSF CSP for 10 weeks exploring sustainable polymer research working on or adjacent to MN Corn projects.